International Journal of Mechanical Sciences 185 (2020) 105868

Contents lists available at ScienceDirect

International Journal of Mechanical Sciences

journal homepage: www.elsevier.com/locate/ijmecsci

Constitutive parameter identification of CB2001 yield function and its experimental verification using tube hydroforming tests

Ali Khalfallah[a,b,c,*], Marta Cristina Oliveira[a], José Luís Alves[d], Luís Filipe Menezes[a]

[a] CEMMPRE, Department of Mechanical Engineering, University of Coimbra, Polo II, Rua Luís Reis Santos, Pinhal de Marrocos, 3030-788 Coimbra, Portugal
[b] LGM, Ecole Nationale d'Ingénieurs de Monastir, Av. Ibn ElJazzar, 5019 Monastir, Université de Monastir, Tunisia
[c] DGM, Institut Supérieur des Sciences Appliquées et de Technologie de Sousse, Cité Ibn Khaldoun, 4003 Sousse, Université de Sousse, Tunisia
[d] CT2M, Department of Mechanical Engineering, University of Minho, Campus de Azurém, 4800-058 Guimarães, Portugal

ARTICLE INFO

Key words:
Tube hydroforming
Constitutive parameter identification
Plastic anisotropy
Corner fill test
Thickness distribution
Finite element analysis

ABSTRACT

The present work focuses upon the use of tube hydroforming into square cross sectional-die as validation test for new constitutive parameter identification strategy. It presents how a developed identification startegy using a reduced set of experimental data in conjuction with some generated artificiel input data are proficient to identifiy the anisotropy parameters of an advanced Cazacu & Barlat yield criterion CB2001, which requires a large number of experimental data for its calibration. Two tubular materials are investigated, namely: mild steel S235 and AA6063 aluminum alloy, which manifest miscellaneous plastic behaviors. The concordance between numerical and experimental thickness distribution along a profile of the hydroformed part into cross sectional-die are the main facing challenges for the validation of the proposed calibration strategy. The analysis of the present findings reveals good agreement between numerical simulation and experimental results. Eventually, the proposed approach is a user friendly-identification strategy and effective method, which can be applied for the calibration of recent developed yield functions for better modeling anisotropic plastic behavior of sheet and tube metals and then could likely widespreadly used in research laboratories as well as in automative industry.

1. Introduction

The tube hydroforming (THF) is a process used to deform initial circular tubes to a various tube cross-section shapes, and among those geometries, the quadrilateral cross-section profiles. The THF process is extensively applied in the automotive and aerospace industries using different materials having reduced weight to stiffness ratio (e.g. aluminum alloys and magnesium-based alloys among others) [1,2] in order to reduce weight components, to decrease energy consumption and to enhance structural strength and stiffness concurrently [3,4]. Thus, nowadays, an extensive number of car parts having complex and non uniform cross-section geometries are produced by tube hydroforming technology [5]. Tube hydroforming process is a very complex process with respect to the mechanical characterization of highly anisotropic tubular materials with limited formability, friction estimation and process control difficulties, among others. Considering the material characterization, the uniaxial tensile test can be adopted to obtain the mechanical properties along axial direction; however for highly anisotropic tubes; the properties along axial and circumferential directions are quite different. Besides, it is more intricate to get accurate experimental results from tensile tests performed along other directions. Moreover, in tube hydroforming process the material undergoes biaxial stress state; and the anisotropic feature of extruded or roll-formed tubular materials is related to their formability and plastic behavior, which are also dependent on the stress state. Therefore, hydro-bulging test in which tubes deform in similar stress state as in the hydroforming process has become one of the successful and widely used testing methods for the characterization of tubular materials. Lately, different equipment and testing methods have been developed and applied for the determination of biaxial stress-strain curves of tubular materials subjected to biaxial stress state. Generally, free hydro-bulging test with fixed tube-ends is the most employed test for determining the plastic flow behavior of tubes, because it is relatively easy to perform [6,7]. Additionally, this test realizes measurement results more stable and comparable. In order to obtain the tubular material flow stress, which is determined from hydro-bulging test results, the stress components that define the biaxial stress state are not explicit, but derived from analytical models based on the plastic membrane theory and using approximations of the bulge profiles. Fuchizawa [8] proposed a mathematical model in which the profile at the apex of the free bulged zone was presumed as circular arc. Based on the thin-walled theory, and in order to appreciate the formability and quality of tubular materials, Sokolowsky et al. [9] developed a method comparable to the one proposed by Fuchizawa.

* Corresponding author.
E-mail address: ali.khalfallah@dem.uc.pt (A. Khalfallah).

https://doi.org/10.1016/j.ijmecsci.2020.105868
Received 3 October 2019; Received in revised form 20 May 2020; Accepted 4 June 2020
Available online 6 June 2020

Hwang [7] proposed an analytical model in which the tube profile of the free bulged zone was assumed as elliptical arc and considering the material anisotropy. Liu et al. [10] and Saboori et al. [2] determined the flow stress of a set of tubular materials using Digital Image Correlation technique to extract the coordinates of the bulge profile in order to calculate the axial and circumferential radii of curvature using curve fitting- methods. Although, the later measurement method provides accurate experimental results, since all data is obtained from a single test; however, the proposed analytical models are based, either on isotropy behavior assumption or on simple anisotropy models. Thus, considering these simple analytical models, the accurate description of the formability of tubular materials with highly pronounced plastic anisotropy is challenging. [2,6,7,11,12]. Moreover, the validity of the proposed approaches was assessed by comparing numerical simulation using the derived flow stress and the experimental results obtained from hydro-bulging test itself. In other words, the hydro-bulge tests are simultaneously used for the parameter identification and the validation of these models. Nevertheless, the main challenges facing these methods is the determination of flow stress curves that can be utilized as input data in finite element codes to predict numerical results in agreement with experimental ones in the framework of the industrial tube hydroforming process.

Square or rectangular cross-sectional dies are commonly obtained by tube hydroforming process for manufacturing automobile parts (e.g., Engine cradles, exhaust systems, rear axles, etc.). The main performed studies concerning the tube hydroforming of circular-section tubes expanded into die cavities of quadrilateral cross-sections are concisely outlined. Woo proposed numerical analysis of the hydro-bulging process of tube under internal pressure and axial force [13]. Koç and Altan developed two-dimensional FEA model to examine the plastic behavior of tubes expanded into simple die cavities [14]. Manabe and Amino studied the effects of stress ratio, hardening exponent, anisotropy coefficients and friction coefficient on the thickness distribution and failure location of hydroformed tube into square cross sectional-die using combined internal pressure and axial force [15]. Kridli et al. used a two-dimensional plane-strain finite element model to evaluate the effects of material properties and die geometry on the selection of hydroforming process parameters. The effects of the strain-hardening exponent, initial tube wall-thickness, and die corner radii on corner filling and thickness distribution of the hydroformed tube were discussed [16]. Hwang and Chen proposed a model considering the sticking friction mode to predict the forming pressure and thickness distribution of formed parts during expansion in a rectangular die [17]. Later, Hwang and Chen proposed analytical model, which takes account of the sliding friction coefficient between the outer tube surface in interaction with the die interface, in order to investigate the plastic deformation behavior of tubular materials expanded into a square cross-sectional die. They discussed the effects of the friction coefficient upon the forming pressures and thickness distribution by comparing finite element method results with those predicted by their analytical models [18]. Rama et al. proposed a two-dimensional numerical model for the simulation of hydroforming expansion of tubular cross-sections without axial feed [19]. Yuan and Wang conducted experimental work and numerical simulation to scrutinize hydroforming of automotive rectangular-section structural parts. They studied the effect of loading paths on the thickness distribution and failure, that automobile prototype parts are subjected to [20]. Orban and Hu developed an analytical model to determine the variation of stresses and strains against the increment of internal pressure applied to expand the tube into a square cross-sectional die. They conducted a parametric study on the effects of the interface friction coefficient and the material properties on the thickness distribution along the tube wall [21]. Xianghe et al. proposed an analytical model to study the effects of the friction coefficient, the strain-hardening exponent and anisotropy coefficient on the thickness distribution of square-sectional hydroformed workpieces [22]. They assessed their model by comparing analytical and simulation results with the experimental ones. Later, Xianghe et al. explored the effects of loading paths, friction coefficient and die angles of a trapezoid-sectional die on the hydroforming process and on the thickness distribution along the unsupported wall of the tubular cross section parts [23]. Recently, Abdelkafi et al. carried out only an experimental study using corner filling test and applying merely internal pressure loading for expanding copper tubes (CU-DHP) into square, rectangular, trapezoidal and trapezoid sectional dies. The thickness distribution profiles were measured in both dry and lubricated conditions. For all the hydroformed parts, the authors reported that the thinning was significantly reduced compared to the dry condition, when Teflon lubricant was employed over the interface tube/die [24]. Thereafter, Abdelkafi et al. used Orban and Hu analytical model [21] to derive the friction coefficient between the hydroformed part and the squared cross-sectional die during corner fill test of copper tube. They compared predicted analytical results with three-dimensional and two-dimensional finite element simulations against the experimental response of thickness distribution at the tube mid-span profile across the square cross-sectional shape. They found that a friction coefficient of 0.1 was the more appropriate value to validate predicted results [25]. Later, Abdelkafi et al. used the pin-on-disk test and Orban-Hu model to evaluate friction coefficient between hydroformed part contact surface against the rectangular, trapezoidal, and trapezoid-sectional dies. They declared that their main goal was to assess the theoretical model ability for the prognosis of the friction conditions in comparison with the pin-on-disk test results. Using Orban -Hu model, the authors found that the friction coefficient values are 0.05 and 0.25 obtained for lubricated and dry tests, respectively [26]. Freshly, Venkateshwar Reddy et al. studied the effect of coefficient of friction between the interface tube/die on the thickness distribution profile using numerical simulations of the corner fill test. They carried out pin-on-disk experiments on SS304 tubes to find the wear and friction coefficient. They reported that the friction coefficient is varying in the range of 0.05 to 0.12 [27].

For relatively recent forming processes and for less mastered ones, the finite element method emerges as an efficient tool to cut costs and decreases the development cycle time invested in trial and error methods and then restricts the number of prototypes. However, finite element simulation results are dependent on the diversity and accuracy of the used input data, usually derived from experimental tests and on the competence of the considered constitutive equations (i.e., advanced yield criteria involve large number of anisotropy coefficients) to accurately reproduce effective material behavior. Although, in the last few years, advanced anisotropy yield criteria have been increasingly developed and used to simulate sheet metal forming [28,29,30,31]; however, it is surprising that the use of advanced constitutive equations in finite element simulations of tube hydroforming process is still very limited [32]. The lack of widespread use of recently developed constitutive equations for describing plastic deformation behavior of highly anisotropic tubular materials (i.e., aluminum and magnesium alloys) is likely attributed to the complexity procedures of extracting the necessary required material properties from circular-section tubes. Such shortcomings make the parameter identification of advanced yield criteria using tubular materials is an intricate charge.

Besides, the limitation of analytical models used to determine the tubular material properties, has incite the development of more reliable identification methods, such as inverse techniques [33], which are used to achieve rugged parameter identification of material properties. Xu et al. developed an adaptive inverse finite element method used for parameter identification of anisotropic tubular materials [34]. An inverse energy method was proposed by Strano et al. to derive the stress-strain curve of isotropic tubular materials [35]. Zribi et al. have applied an identification method based on the coupling of experimental free bulge and tensile tests with finite element simulation to derive the flow stress and Hill48 anisotropy coefficients of mild steel and aluminum tubular materials [6,36]. One can note that, robust inverse techniques are herein solely limited to identify the parameters of restrictive constitutive equations, such as, von Mises and Hill48 yield functions. Obviously, they

are insufficient to describe the complex anisotropic plastic deformation behavior of aerospace alloys used in tube hydroforming process [2].

In the present work, we propose on one hand, an efficient identification method using a reduced set of experimental data measured from three directional tensile tests along with the free hydro-bulging test. The constitutive parameter identification of CB2001 yield criterion [37] is carried out using specific calibration strategy for a better description of the anisotropic plastic deformation behavior of tubes, namely: S235 a mild steel and AA6063 an extruded tube of aluminum alloy. The calibration strategy is based upon the use of restricted available experimental data complemented with generated artificial data. The artificial data are generated from less flexible yield functions (i.e., including few anisotropy coefficients) to compensate the missing experimental data needed for calibration procedure of sophisticated yield criteria.

On the other hand, the identified parameters are used as input data to simulate the expansion of circular tube into a square cross-sectional die, a typical hydroforming test, to validate the proposed CB2001 calibration strategy and to check its effectiveness for describing the anisotropy of the studied tubular material behaviors. The predicted wall thickness distribution profile obtained from the hydroforming into square cross-section is compared to experimental results.

2. Experimental details

In the present work, experimental tube hydroforming tests were carried out using a made home-tooling machine. To characterize the plastic deformation behavior of anisotropic tubular materials, free bulge testing were performed on tubes made of S235 mild steel and AA6063 aluminum alloys, along with uniaxial tensile tests. The investigated tubes have an outer diameter equal to 50 mm. The measured initial wall-thicknesses are equal to 1.07 mm for S235 and 2.04 mm for AA6063 aluminum alloy.

The free bulge testing outputs are the applied internal pressure versus the bulge height at the top of the dome. By transforming this response to stress –strain curve, it is possible to derive the biaxial stress state defined by the stress ratio $\alpha = (\sigma_{22}/\sigma_{11})$ and then the two stress components σ_{11} and σ_{22}, that the tube experienced at the top of the dome along the axial and circumferential directions, respectively.

On the other hand, three tensile tests were carried out along three directions, 0º, 45º and 90º with respect to a referential direction (i.e., the tube axial direction). Further experimental details were given elsewhere [6].

Table 1 summarizes the experimental results obtained from tensile tests, which represent a subset of the complete dataset used in the parameter identification of the CB2001 yield function.

As above mentioned, the yield stresses of anisotropic tubular materials are obtained from tensile testing on samples cut in three directions with respect to the axial direction, (i.e., referential direction) from flattened tube. The flattening operation alters the initial yield stresses, as a result the measured initial yielding stresses are error affected [6,11]. It has been established from the latter references, that mechanical properties of tensile tests carried out on samples cut off a tube and tube-flattened sheet are similar after at least 5% of plastic deformation. Thus, in order to reduce inaccuracies on the determination of experimental initial yield stresses, an equivalent plastic strain of 10% was chosen for which these stresses were measured.

Swift strain hardening law is selected to represent the flow stress of the S235 and AA6063, respectively.

$$\overline{\sigma} = K(\varepsilon_0 + \overline{\varepsilon}_p)^n \tag{1}$$

where K, ε_0 and n are the constants of Swift's strain hardening relationship. The experimental tensile data in the tubular axial direction were fit to Swift's law, producing these material parameters for the mild steel S235: K = 722.7 MPa, pre-strain $\varepsilon_0 = 0.0171$ and strain hardening exponent n = 0.384. For AA6063 aluminum alloy, the fitting of Swift's law with data points provides the following material parameters: K = 178.71 MPa, pre-strain $\varepsilon_0 = 0.0018$ and strain hardening exponent n = 0.202.

In order to validate the model identification for predicting the plastic behavior of tubular materials, a square cross-sectional die was manufactured, where the side of the square is 50 mm equal to the external tube's diameter and the length is 60 mm. The die is placed within the spacer region between the two guiding dies, which are used for supporting the tube extremities. Two horizontal plungers locked the tube ends. For the S235 mild steel, the internal pressure is increased gradually from 0 up to 50 MPa and for the AA6063 aluminum alloy, the pressure was increased from 0 till 18 MPa. The experimental thickness distribution at the mid-span profile across the square sectional shape at one corner of the hydroformed part was recorded and average values were considered. During the experimental tube hydroforming test into the square cross-sectional die, lubrication of die/tube interface is generously guaranteed, and the considered friction coefficient was 0.08 assumed for test simulation purpose.

3. CB2001 yield criterion

The advanced anisotropic yield criterion denoted by CB2001 was proposed by Cazacu and Barlat in 2001 [37]. They have proposed a method to extend the Drucker's isotropic yield function expressed in terms of the invariants of the stress deviator to obtain a version of anisotropic yield criterion. The CB2001 orthotropic yield function is expressed as follows:

$$\left(J_2^0\right)^3 - c\left(J_3^0\right)^2 = 27\left(\frac{\bar{\sigma}}{3}\right)^6 \tag{2}$$

The following equations express the second and third generalized invariants of the stress deviator tensor:

$$J_2^0 = \frac{a_1}{6}(\sigma_{11}-\sigma_{22})^2 + \frac{a_2}{6}(\sigma_{22}-\sigma_{33})^2 + \frac{a_3}{6}(\sigma_{11}-\sigma_{33})^2 + a_4\sigma_{12}^2 + a_5\sigma_{23}^2 + a_6\sigma_{13}^2 \tag{3}$$

$$\begin{aligned} J_3^0 = {} & \frac{1}{27}(b_1+b_2)\sigma_{11}^3 + \frac{1}{27}(b_3+b_4)\sigma_{22}^3 + \frac{1}{27}(2(b_1+b_4)-b_2-b_3)\sigma_{33}^3 \\ & - \frac{1}{9}(b_1\sigma_{22}+b_2\sigma_{33})\sigma_{11}^2 - \frac{1}{9}(b_3\sigma_{33}+b_4\sigma_{11})\sigma_{22}^2 \\ & - \frac{1}{9}((b_1-b_2+b_4)\sigma_{11}+(b_1-b_3+b_4)\sigma_{22})\sigma_{33}^2 \\ & + \frac{2}{9}(b_1+b_4)\sigma_{11}\sigma_{22}\sigma_{33} - \frac{1}{3}(2b_9\sigma_{22}-b_8\sigma_{33}-(2b_9-b_8)\sigma_{11})\sigma_{13}^2 \\ & - \frac{1}{3}(2b_{10}\sigma_{33}-b_5\sigma_{22}-(2b_{10}-b_5)\sigma_{11})\sigma_{12}^2 \end{aligned}$$

Table 1
Experimental data obtained from tensile tests for the S235 and AA6063 tubular materials: *r*-values and yield stresses are measured at an equivalent plastic strain ($\bar{\varepsilon}^{pl} = 10\%$); these results are measured along three directions relative to the tube's axial direction as the reference direction of orthotropy.

Material	*r* – values along three directions			Normal anisotropy	Yield stresses along three directions at $\bar{\varepsilon}^{pl} = 10\%$		
	r_0	r_{45}	r_{90}	$\bar{r}$	σ_0(MPa)	σ_{45}(MPa)	$\sigma_{90(MPa)}$
S235	**1.48**	**0.92**	**1.51**	**1.20**	**442.9**	**467.4**	**438.2**
AA6063	**0.59**	**0.83**	**0.79**	**0.76**	**112.8**	**77.4**	**81.8**

$$-\frac{1}{3}\left(\left(b_6+b_7\right)\sigma_{11}-b_6\sigma_{22}-b_7\sigma_{33}\right)\sigma_{23}^2 + 2b_{11}\sigma_{12}\sigma_{23}\sigma_{13} \quad (4)$$

The coefficients $a_k(k = 1,..6)$, $b_k(k = 1,..11)$ and c are CB2001 anisotropy parameters. The isotropy conditions reduce all the anisotropy parameters to unity. In the assumption of plane stress condition, commonly adopted for thin-walled parts, the eighteen independent anisotropy parameters of CB2001 are reduced to eleven parameters [37].

4. Calibration of the CB2001 yield criterion

As it is well-known, for parameter identification procedures, the number of experimental data should be equal or greater than the number of coefficients to identify. In latter cases, optimization algorithms are applied to minimize an objective function, usually named cost function, which defines the gap between experimental data and model's prediction. Whenever, experimental input data is insufficient to identify model's parameters; herein we put forward several options and scenarios to compensate the lack of experimental results. Foremost, when it is likely possible to conduct experimental tests, then obviously, the ideal solution is to substitute the missing tests by current results and therefore complete the needed set of experimental data to perform the parameter identification procedure. Alternatively, using trivial parameters based on simple assumptions, whenever it is justified, (such as using isotropic parameters) or material properties collected from literature might fix the lack of experimental data. Otherwise, predicted parameters based on advanced or microstructural models outputs [38] can be successfully used to fulfill the experimental missing data. Essentially, the identification of 11 anisotropy parameters of CB2001 (assuming a plane stress state), requires at least 11 experimental input data. Usually, the CB2001 calibration is performed using 7 directional tensile stresses, 7 directional r-values, the balanced biaxial yield stress and the balanced biaxial strain ratio r_b-value [39], as usually practiced for anisotropic sheet metals. However, in this current study, the available experimental data is less than what is required to conduct the parameter identification, since for tubular materials the measurement of directional mechanical properties is an intricate task. So, in this framework, we put forward a methodology for CB2001 calibration that uses generated directional yield stresses and r-values from the identification of four anisotropy coefficients (case of plane stress condition) of Barlat et al. yield criterion, proposed in 1991 and denoted by Yld91 [40]. Three off-axes tensile tests provide three experimental directional yield stresses ($\sigma_{0°}$, $\sigma_{45°}$, $\sigma_{90°}$) and three r-values ($r_{0°}, r_{45°}, r_{90°}$), which are largely sufficient to calibrate the four anisotropy coefficients of Yld91 criterion. Using Yld91 anisotropy coefficients, one can generate several directional yield stresses and r-values. The generated data are labeled "artificial but meaningful" experimental data, since they are utilized to compensate the incomplete experimental data, as proved by Khalfallah et al. [41]. From the generated set of results, one can choose the directional stresses and r-values to complete the missing data with at least eleven input data to identify the anisotropy parameters of the CB2001 yield criterion. Meanwhile, it is also possible to generate equibiaxial stress σ_b and equibiaxial r_b-value [28]. Despite that these latter results are very useful for better description of material behavior at the equibiaxial point on yield surface, the experimental tests that provide such results are usually unavailable in industrial or research laboratories. Since, in the condition of plane stress state, the number of anisotropy coefficients of Yld91 are only four parameters, thus it is considered as a weak flexible yield criterion when it is compared to more flexible yield functions which involve high number of anisotropy coefficients. The deficiency of Yld91 flexibility is depicted by its failure to describe simultaneously the anisotropy of the initial yield stresses and the anisotropy of plastic strains, especially for highly anisotropic materials, such as aluminum alloys [42]. However, it has been found that by tuning differently weighting factors involved in the expression of cost function, one could generate either yield stresses or r-values in good agreement with experimental data. In order to generate yield stresses, the weighting factors assigned to three experimental yield stresses are higher than the weighting factors allocated to the r-values. In the opposite case, the three experimental r-values are privileged compared to the experimental yield stresses and then the weighting factors assigned to the experimental Lankford coefficients are increased [39].

Additionally, as it is well-known, in tube hydroforming process a biaxial stretching mode is the most relevant strain path. Nevertheless, only simple tensile tests are no longer sufficient for precise calibration of advanced yield criteria, because in the zone of the biaxial stress states, the yield locus is likely undecided. Therefore, the free hydro-bulging test is actually the useful experimental test to provide information about the stress states that undergo hydroformed tubes at the apex of the dome. Consequently, including biaxial stress components along with uniaxial tensile tests results as input data in the calibration of CB2001 yield criterion is the proposed identification strategy for proper description of the material behavior by the CB2001 yield function in tube hydroforming process.

The biaxial stress state, encountered in the free bulge test, is defined by stress components σ_{11} and σ_{22} which are deduced from pressure vs. bulge height curve at the pole of the dome. Where σ_{11} and σ_{22} are the stress components in the axial and hoop directions, respectively. These stress components are derived from FE simulations of free hydro-bulging test using the stress-strain curve, which is obtained from the experimental pressure vs. bulge height curve. A well-known methodology is applied for determining the stress-strain curve from experimental pressure vs. bulge height curve. Further details regarding this method are elsewhere in Refs. [2,10].

Table 2 lists material properties of the S235 and AA6063, utilized for the calibration of the CB2001 yield criterion. As referred above, the yield stresses are obtained for an equivalent plastic strain of 10% in order to decrease inaccuracies on material experimental results, because tensile samples are cut from flattened tube specimens and such operation affects the initial yield stresses. However, Lankford coefficients are assumed less sensitive to pre-strains than yield stresses. The conventional parameter identification of anisotropy coefficients is formulated as non-linear optimization problem. The target solution represents the global minimum of a cost function which defines the difference between the experimental data and the calculated results predicted by the model. The following cost function is usually considered in the calibration of yield criteria:

$$Costfunction(x) = \sum_i w_i\left(\frac{\sigma_\alpha^{cal}(x)}{\sigma_\alpha^{\exp}}-1\right)^2 + \sum_i w_i\left(\frac{r_\alpha^{cal}(x)}{r_\alpha^{\exp}}-1\right)^2 + + w_i\left(\frac{\sigma_{11}^{cal}(x)}{\sigma_{11}^{\exp}}-1\right)^2 + w_i\left(\frac{\sigma_{22}^{cal}(x)}{\sigma_{22}^{\exp}}-1\right)^2 + w_i\left(\frac{r_b^{cal}(x)}{r_b^{\exp}}-1\right)^2 \quad (5)$$

where x is the solution of the optimization problem and represents the unknown anisotropy coefficients of CB2001, $\sigma_\alpha^{\exp}$ and $r_\alpha^{\exp}$ are the experimental yield stresses and r-values including the artificial data obtained in a particular direction α with respect to referential orientation. $\sigma_{11}^{\exp}$ and $\sigma_{22}^{\exp}$ are the experimental stress components that define the biaxial stress state and obtained from free bulge test. $r_b^{\exp}$ is biaxial r-value, which is a generated value (i.e., artificial data). σ_α^{cal}, r_α^{cal}, σ_{11}^{cal}, σ_{22}^{cal} and r_b^{cal} are the corresponding calculated value according to the CB2001 yield criterion. w_i are the weighting factors which can be tuned to privilege any chosen experimental data against any others. The weighting factors are used to monitor the optimization procedure and therefore influence the identified solution. The downhill simplex algorithm is herein used to minimize the cost function (Eq. 5). It is a derivative free method, which is useful to avoid falling down into local minima of the cost function. To guarantee global optimized solution, the identification procedure is repeated a quite number of times starting at each run from different set of initial solution. It has been noted that one optimal solution

Table 2
Mechanical properties used for the calibration of CB2001 yield criterion for the S235 and AA6063 tubular materials (bold font: true experimental data).

Type of mechanical test	Tubular material properties	Type of data	S235	AA6063
Tensile test	r_{0°	True	**1.48**	**0.59**
	r_{30°	Artificial	1.04	0.74
	r_{45°	True	**0.92**	**0.83**
	r_{60°	Artificial	1.05	0.85
	r_{90°	True	**1.51**	**0.79**
	σ_{0° (MPa)	True	**442.9**	**112.8**
	σ_{30° (MPa)	Artificial	457.0	82.9
	σ_{45° (MPa)	True	**467.4**	**77.4**
	σ_{60° (MPa)	Artificial	457.4	77.3
	σ_{90° (MPa)	True	**438.2**	**81.8**
	r_b	Artificial	0.98	0.78
Free bulge test	σ_{11} (MPa)	True	**301.3**	**62.0**
	σ_{22} (MPa)	True	**560.4**	**114.7**

Table 3
Anisotropy parameters of CB2001 yield criterion for S235 and AA6063 tubular materials.

Anisotropy Parameters of CB2001	S235	AA6063
a_1	1.13118	1.45472
a_2	1.00108	1.95821
a_3	0.99977	−0.66596
a_4	0.87021	1.78162
b_1	0.94411	0.90497
b_2	3.23771	2.32797
b_3	3.50876	0.33589
b_4	−0.56500	−1.29223
b_5	0.30143	2.55353
b_{10}	0.39091	3.27848
c	0.33381	−2.68147

is obtained (i.e., the global minimum of the optimization problem is attained).

Table 3 lists, for S235 and AA6063 materials, the identified anisotropy coefficients of the CB2001 yield criterion. These anisotropy parameters represent the global optimal solution after solving the parameter identification problem.

Figs. 1a and 2a display the predicted profile of *r*-values and yield stresses at an equivalent strain of $\bar{\varepsilon}^{pl} = 10\%$ for both tubular materials. To distinguish between true experimental data and artificial data, different symbols are used in the plots. It is clearly shown that the CB2001 yield criterion is able to properly describe the evolution of plastic strains and stresses anisotropy. Figs. 1b and 2b display the predicted yield surfaces at onset of the plasticity and at an equivalent plastic strain of 10%. The experimental results are also represented on these plots. Moreover, the latter figures clearly depict that the biaxial stress state at the apex of the bulged area is perfectly captured by the constitutive equation. Such good accordance is evident owing to the higher flexibility of the CB2001 yield criterion and by virtue of the large number of anisotropy parameters, which includes the artificial data to enable efficiently the calibration of CB2001, particularly used to describe the anisotropy behavior of tubular materials, such as AA6063 aluminum alloy.

5. Finite element analysis of tube hydroforming tests

The finite element simulation of tube hydroforming tests are carried out using the DD3IMP in-house finite element software, which has been developed to simulate sheet metal forming processes [43]. Owing to its flexibility, the DD3IMP code was simply accommodated to simulate tube hydroforming tests, namely the free bulge test and the tube hydroforming into square cross-sectional die. The code uses a fully implicit algorithm of Newton-Raphson within a single iterative loop. The deformation kinematic is described by an updated Lagrangian scheme and contact friction is governed by the Coulomb's classical law treated with a mixed formulation using the augmented Lagrangian approach. The contact takes place between the tube and the rigid bodies (i.e., dies) modeled with Nagata patches [44]. The deformable parts are meshed with 8-node hexahedral solid finite elements using selective reduced integration (SRI).

Considering the geometric, loading, boundary conditions and material symmetries, one eighth of the entire part was modelled in the purpose of decreasing computational span. Fig. 3a shows the 3D finite element model used for the free bulge test simulation and Fig. 3b illustrates 3D finite element model built for the numerical simulation of tube hydroforming into the square cross-sectional die. In both cases, the applied internal pressure is defined as a linear time-dependent curve.

5.1. FE simulation of free bulge test

3D finite element model of the free bulge test consists of two parts. The first one is the tube modeled as deformable body. Two mesh sizes are considered after a sensitivity of the mesh refinement to discretize the deformable part in order to converge to accurate FE solution in a reduced computational time. Mainly, the central bulging region is meshed with element size of 1 mm x 1.3 mm in the hoop and axial tube directions. Two layers of finite elements are used through the thickness and found sufficient after a convergence analysis of the number of finite element layers on accuracy of thickness results. Coarse mesh is applied to the remaining part of the tube, i.e., tube zones, which are in contact with the tube guiding die, modelled as rigid body. Tube guiding die serves to control the free bulged area and to retain the tube's extremities during deformation. The die entrance radius is set to 7.5 mm and the width of the free bulged area is set to 60 mm. The tube outer diameter is 50 mm for both tubular materials. The initial thickness is 1.07 mm for S235 and 2.04 mm for AA6063 as committedly obtained from experimental measurements.

Fig. 4 shows the comparison between experimental curves along with the numerical results of the bulge height plotted against the internal pressure for both tubular materials S235 mild steel and AA6063 aluminum alloy. These numerical results are obtained from finite element simulation of the free bulge test, using the identified anisotropy parameters of CB2001 yield criterion, given in Table 3, as input data in the numerical simulations. One can see the good agreement between the experimental points and the predicted curves. Subsequently, this confirms at least for the free bulge test, that the CB2001 is a suitable constitutive equation and the identification of its anisotropy parameters are quite accurate to describe the stress path during the free bulge test as beforehand displayed in Figs 1b and 2b.

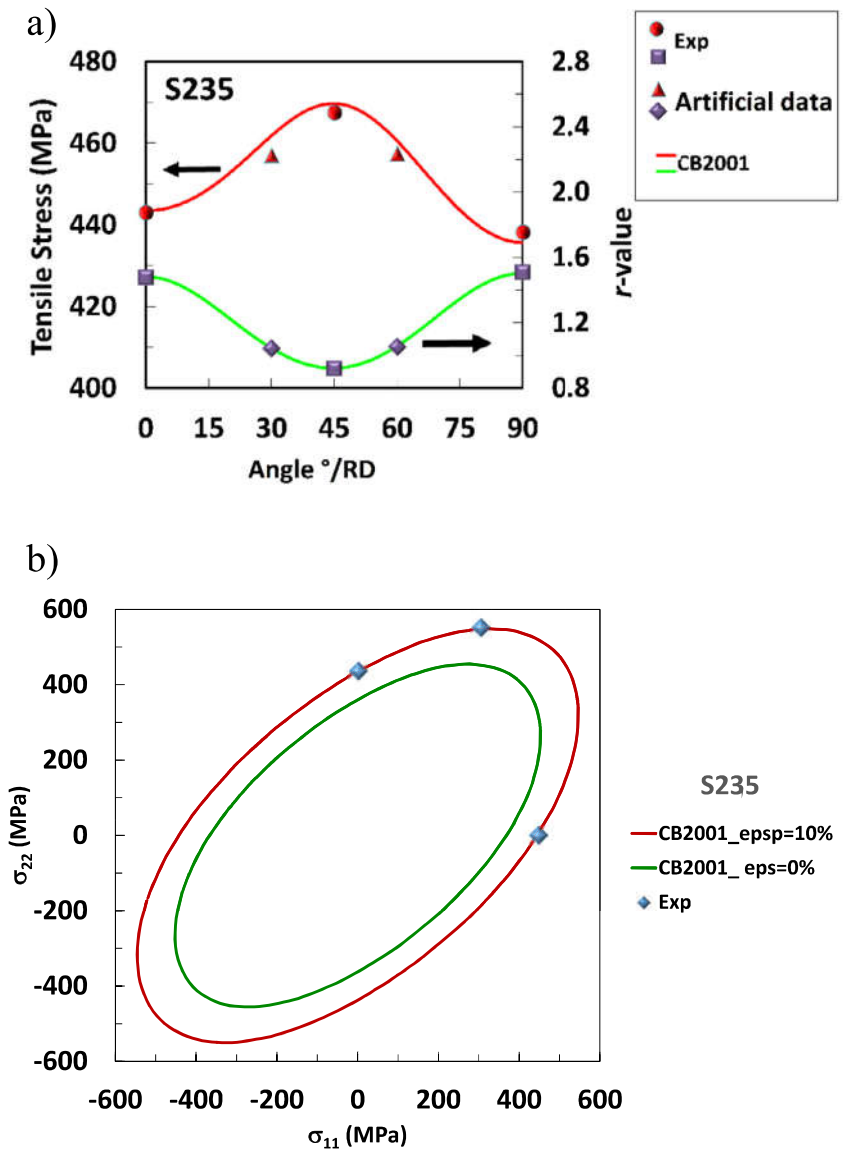

Fig. 1. Predicted results using CB2001 yield criterion against experimental ones obtained for the mild steel S235: a) *r*-values and tensile stresses obtained at an equivalent plastic strain of $\bar{\varepsilon}_p$= 10%. Different symbols were used in the plots to distinguish between true experimental data and artificial one; b) yield surface in σ_{11},σ_{22} space (contours for σ_{12} = 0) obtained for an equivalent plastic strain of $\bar{\varepsilon}_p$= 10% along with the calculated initial yield surface, i.e., $\bar{\varepsilon}_p$= 0.

5.2. FE simulation of tube hydroforming into square cross-sectional die

3D finite element model of the square cross- sectional die consists of two parts. The first part is the tube (deformable part). The discretization of the tube of an outer diameter of 50 mm is made with a combination of two sized meshes. In order to gain better accuracy of the finite element simulation results, an optimization of the refinement mesh has been carried out. The mid-span region of the hydroformed tube into square cross-sectional cavity is meshed with an element size of 1 mm x 1.3 mm and two layers are used across the thickness; therewith, a coarser mesh is used elsewhere for the deformable part.

The second part of the finite element model is a square cross-sectional die, which is modelled as rigid body and has an edge length equal to 50 mm.

In fact, the square cross-sectional die is obtained from the free bulge test set up by interposing the square cross-sectional die within the space between the dies, which hold and guide the tube throughout the bulging test.

The friction coefficient between the tube/die interfaces is set to the experimental value of 0.08. This value is estimated based on experimental conditions (i.e., experimental hydroforming tests performed with lubrication) and on sensitivity analysis of the friction coefficient on the thickness distribution performed by FE Analysis. The considered friction coefficient is in accordance with the experimental investigations reported in literature [45,46].

The finite element simulation of the square cross-sectional die test for both tubular materials are performed using the identified parameters of the material constitutive equation based on CB2001 yield criterion and isotropic strain hardening law, given in Eqs. (1) and (2). It consists of expanding a tube circular cross-section into a square cross-sectional die. The tube profile along the middle cross-section at one corner of the hydroformed part is shown in Fig. 5. It displays the initial and deformed configuration of one quarter of the tube. The tube hydroforming against the square cross-sectional die permits to distinguish two regions. The segments AB and A'B' correspond to the adhered zone of the tube to the die-wall surface and the segment BB' is accounted for the unsupported part. The tangential points B and B' represent the transition points between stuck zones against the internal wall-die surface and the unsupported regions which are the corner areas. These points are the critical areas, in which an excessive thinning usually occurs [24]. During tube hydroforming process, the successful chief operation consists in bulging out the tube to fit the designed cross-section-die cavity without defects.

The friction between the tube and the die contact surfaces plays an important role in the thickness distribution and uniformity of the tube

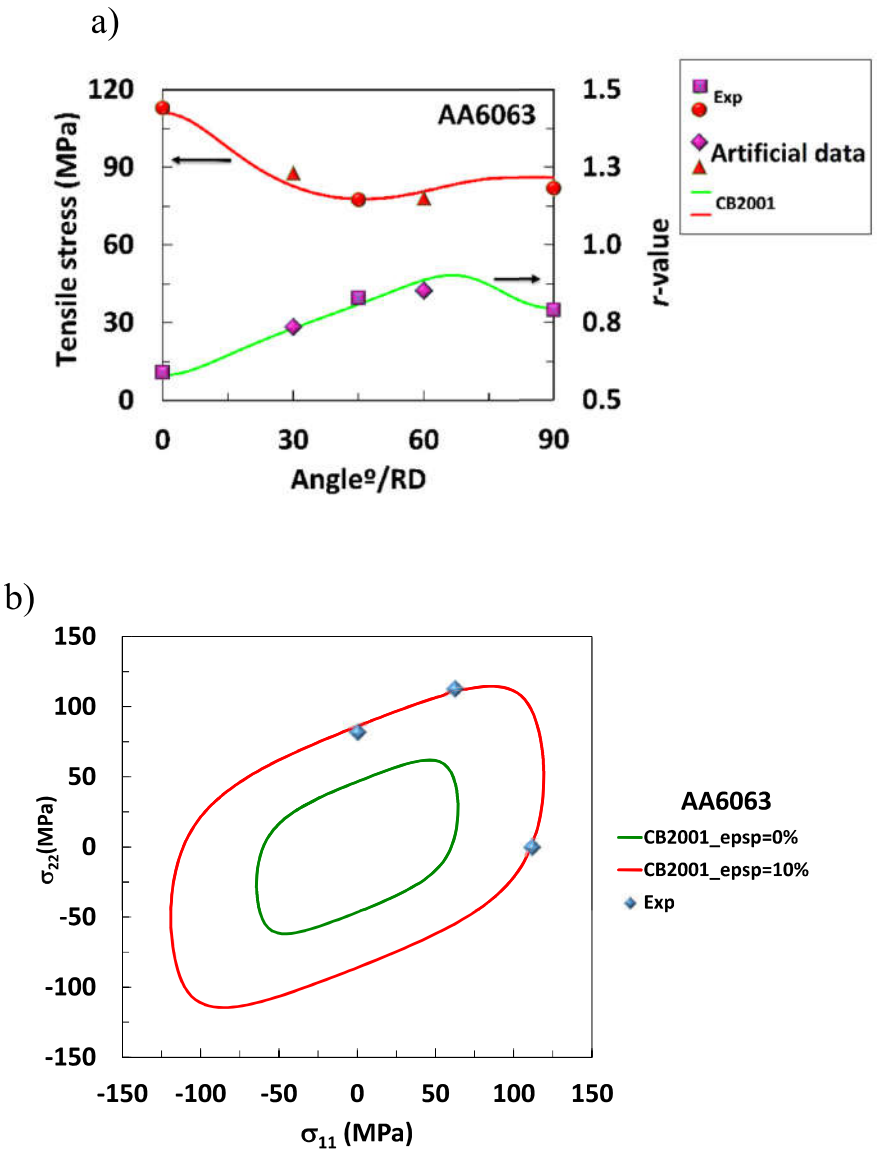

Fig. 2. Predicted results using CB2001 yield criterion against experimental ones obtained for the mild steel AA6063: a) *r*-values and tensile stresses obtained at an equivalent plastic strain of $\bar{\varepsilon}_p$= 10%. Different symbols were used in the plots to distinguish between true experimental data and artificial one; b) yield surface in σ_{11},σ_{22} space (contours for σ_{12} = 0) obtained for an equivalent plastic strain of $\bar{\varepsilon}_p$= 10% along with the calculated initial yield surface, i.e., $\bar{\varepsilon}_p$= 0.

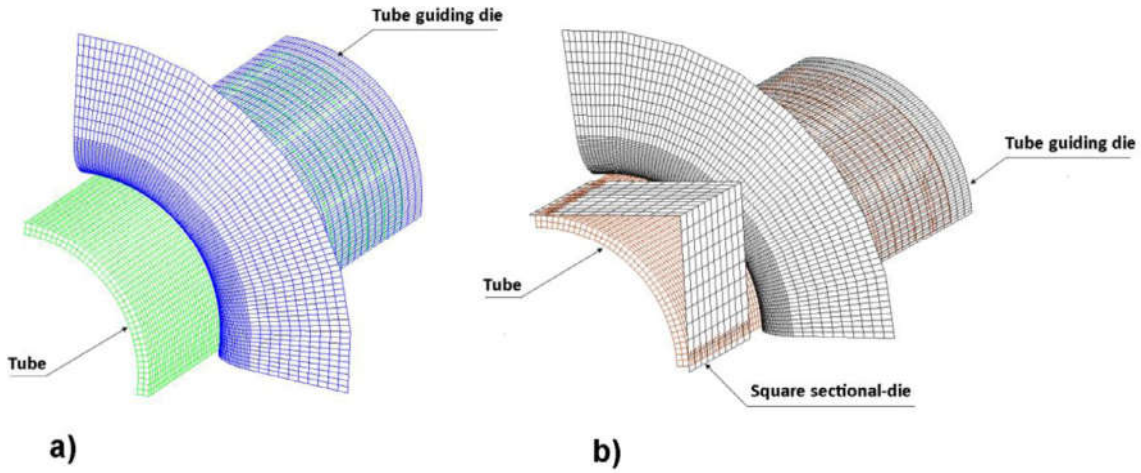

Fig. 3. 3D finite element models for the simulation of: a) free bulge test; b) cross-sectional die test.

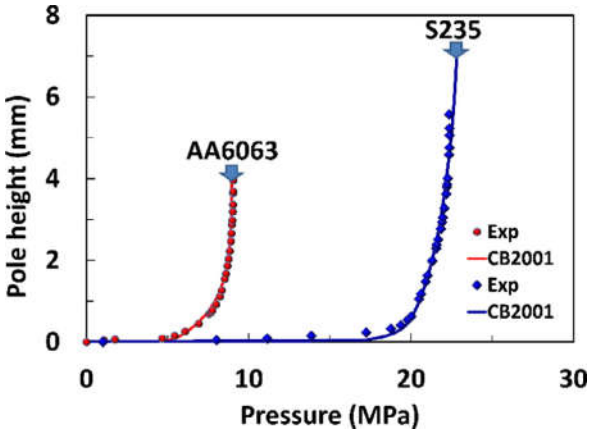

Fig. 4. Comparison between experimental and predicted results using CB2001 model of the free bulge test response (radial deflection vs. internal pressure) obtained for the S235 (blue solid square symbol,"◆") and for the AA6063 (red solid circle symbol,"•").

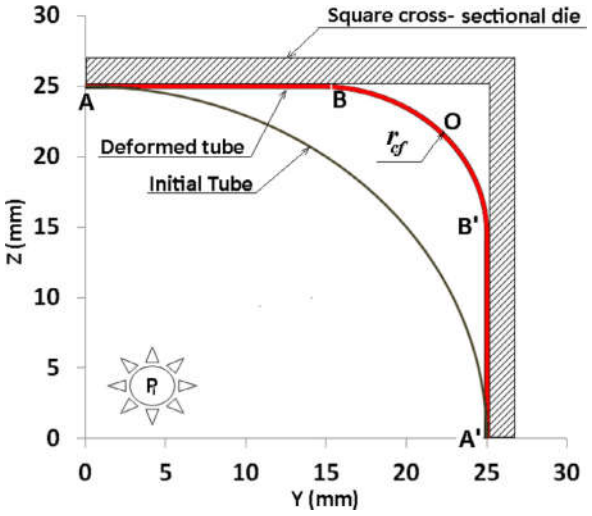

Fig. 5. Tube corner fill of squared cross-section shape before deformation (quarter of circle plotted with black continuous line) and after hydroforming against the square cross-sectional die (plotted with red continuous line). The segments AB and A'B' refer to the adhered zone and BOB' curved line corresponds to the unsupported zone.

hydroforming process. In order to assess effects of the friction coefficient on the thickness distribution, a parametric analysis of the friction coefficient is performed by varying the coefficient from 0 to 0.2. Fig. 6 shows for the S235 and AA6063 tubular materials, the effect of the friction coefficient on the thickness distribution of tube expansion into the square cross-sectional die. It displays the thickness profile at the mid-span of the tube squared cross-section dependent of the friction coefficient. For both studied materials, one can see that, as the friction coefficient increases, the sticking segment AB length is slightly growing and sharp thinning occurs at the transition zones (tangential points B and B') leading to heterogeneous thickness distribution. Since the thinning of the transition zones between straight segments and corners is more serious than the other regions, then earlier necking occurs which is followed by tube fracture at those locations. However, less friction contributes to thickness distribution uniformity. Liu et al. have analyzed by mechanical analysis and numerical simulation the local thinning at the transition region in the tube hydroforming process of the square cross-section [47]. They concluded that higher friction coefficient between tube/die interface leads to a serious local thinning at transition zones, heterogeneous deformation and small corner radius achievement, i.e., difficulties for the tube in fitting the cross-section forming die. Moreover, it was observed that the friction coefficient has less effect on the location of transition points under the same internal pressure, but a small shift of the thinning location is perceived when the friction coefficient augments. Similar findings were obtained herein, as can be seen in Fig. 6. It is worthy to denote that the effect of friction becomes more significant when axial feeding is introduced [48]; then by improving lubrication conditions contributes to an enhancement of the thickness distribution uniformity.

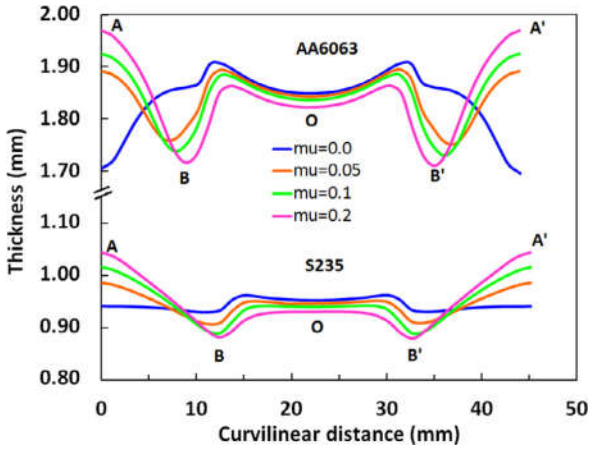

Fig. 6. Effects of friction coefficient (mu varies in the range of 0 to 0.2) on the thickness distribution at the tube's mid-span and along the corner of the squared cross section for AA6063 and S235 tubular materials.

6. Experimental verification of the CB2001 calibration strategy

The experimental verification of the CB2001 calibration strategy is based on the comparison of experimental thickness distribution measured in the mid-span of the expanded tube to the numerical thickness obtained by finite element analysis of square cross-sectional-die test. The anisotropy coefficients listed in Table 3 along with strain hardening constants are used as input data to run finite element simulations.

Fig. 7 shows for the S235 mild steel and the AA6063 aluminum alloy the comparison between the experimental and predicted results using CB2001 yield criterion of the thickness distribution at the mid-span profile of the hydroformed tube into a cross-sectional die.

The internal pressure of 50 MPa and 18 MPa were applied for the steel and the aluminum tubes, respectively. One can see the good accordance between the simulation and the experimental responses. For S235 steel, the root-mean square error between the experimental and numerical curves was estimated at about 1%. In addition, the gap between the thinnest (tangential point B) and thickest point (middle point O) in the unsupported region of the part is less than 5%. This is a good indication of an enhanced thickness distribution uniformity. This is attributed on one hand, to the modest friction coefficient (mu ==0.08) obtained using lubrication of the die/tube interface, and on the other hand to the high hardening exponent (n = 0.384 obtained for S235) and to normal anisotropy coefficient which is about 1.2, which play together a key role in the homogeneity of thickness distribution and then a resistance against severe thinning in the hydroformed workpiece. In contrast to that observed for S235, and notwithstanding some thickness distribution discrepancy between experimental and predicted results, as shown in Fig. 7, it was revealed for the AA6063 aluminum alloy a similar tendency of both curves. The difference was evaluated at a value of about 7%. In addition, the thickness distribution along the unsupported zone is not as uniform as that obtained for the steel material S235. One can observe that the middle point O is not the thickest one along the unsupported zone. This can be attributed to the lower hardening exponent of the AA6063 aluminum alloy (n = 0.202) compared to that

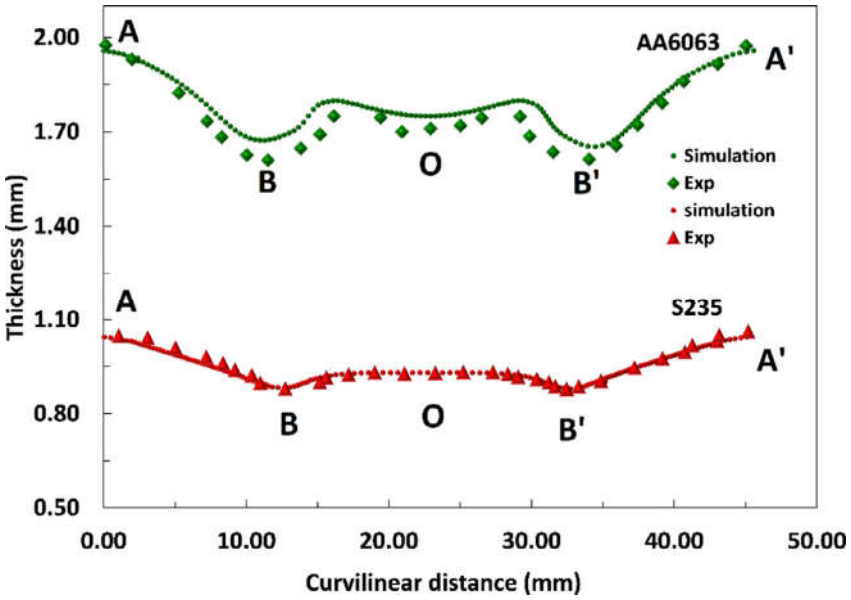

Fig. 7. Comparison of thickness distributions between experimental data and simulation results using CB2001 anisotropic plasticity model along the tube's mid-span of the hydroformed parts into the square cross-sectional die for S235 steel and AA6063 aluminum alloy.

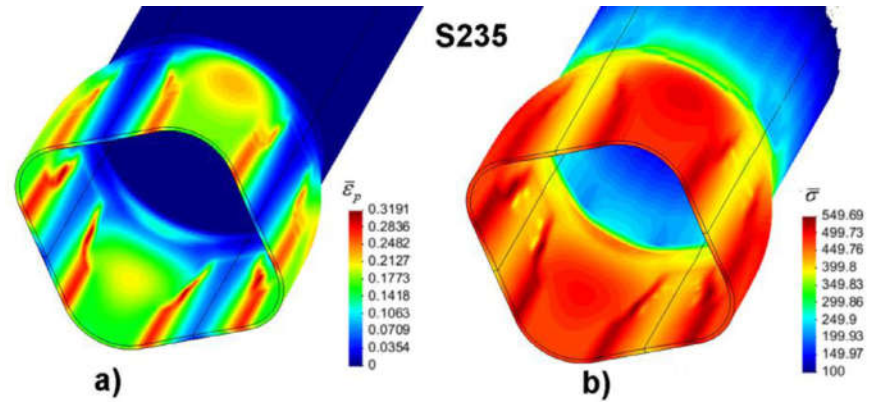

Fig. 8. 3D-numerical simulation results using CB2001plasticity model of hydroformed parts for S235 into a square cross-sectional die obtained for an applied internal pressure of 50 MPa: a) contours of the equivalent plastic strain; b) contours of the equivalent stress.

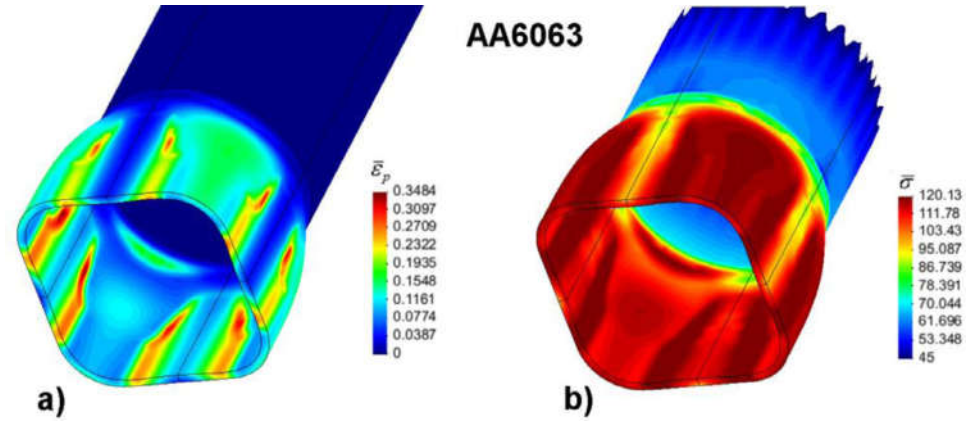

Fig. 9. 3D-numerical simulation results using CB2001plasticity model of hydroformed parts for AA6063 into a square cross-sectional die obtained for an applied internal pressure of 18 MPa: a) contours of the equivalent plastic strain; b) contours of the equivalent stress.

of S235 and also to the low normal anisotropy coefficient ($\bar{r} = 0.76$), and particularly the low anisotropy coefficient in the hoop direction, which is equal to 0.79. Similar conclusions have been reported by Xianghe et al. [22]. Moreover, it is known that an increment of anisotropy coefficient helps material to flow into the bulging zone or the unsupported zone, which supports the improvement of the thickness distribution uniformity. That's likely why for AA6063, the middle point O of the unsupported zone (BOB') in the hydroformed part into a square sectional-die is different to that observed for S235. Figs. 8 and 9 show 3D-numerical simulation results of tube hydroforming, using CB2001 anisotropic plasticity model, into square cross-sectional die with an applied internal pressure of 50 MPa and 18 MPa for S235 and AA6063, respectively. These figures depict the contours of the equivalent plastic strain and equivalent stress within the hydroformed part for both materials. They support the above-mentioned statements regarding the thickness distribution for S235 and AA6063 materials. Consequently, it is recommended that tubes having higher hardening exponent and normal anisotropy coefficients are more efficient for a homogeneous thick-

ness distribution in tube hydroforming processes; moreover, good and munificent lubrication has also important beneficial effect upon quality of hydroformed parts.

7. Conclusion

The experimental characterization of tubular materials, S235 mild steel and AA6063 aluminum alloy as studied cases was carried out using simple tensile test and free bulge test. Simple tensile and free bulge tests were performed to get material anisotropy coefficients and the flow stress parameters. New parameter identification procedure has been achieved in order to identify the CB2001 yield function anisotropy parameters based upon less experimental input data. Tube hydroforming into square cross sectional-die test is used as verification test for the developed method by comparing experimental thickness distribution to finite element results. It has been shown, good agreement between experimental and numerical responses, which confirms the robustness of the developed parameter identification approach and the capacity of the used yield criterion CB2001 to deal simultaneously with the stresses and strains anisotropy of two different tubular material behaviors. In addition, it can be concluded that low friction coefficient along with both higher hardening exponent and normal anisotropy coefficient contribute to better uniformity of thickness distribution in tube hydroforming process. Finally, the main objective of the present work is to come up with a useful parameter identification methodology to help engineers working in plasticity field of thin walled structure industries, to calibrate advanced yield criteria with cut costs by using reduced experimental results.

Declaration of interests

The authors declare that they have no known competing financial interests or personal relationships that could have appeared to influence the work reported in this paper.

CRediT authorship contribution statement

Ali Khalfallah: Conceptualization, Methodology, Investigation, Data curation, Formal analysis, Validation, Writing - original draft, Writing - review & editing. **Marta Cristina Oliveira:** Writing - review & editing, Software, Validation. **José Luís Alves:** Software. **Luís Filipe Menezes:** Software, Supervision.

Acknowledgments

The authors gratefully acknowledge the financial support of the Portuguese Foundation for Science and Technology (FCT) via the projects PTDC/EMS-TEC/1805/2012 and PEst-C/EME/UI0285/2013 and by FEDER funds through the program COMPETE – Programa Operacional Factores de Competitividade, under the project CENTRO-07–0224-FEDER-002001 (MT4MOBI). Currently, the first author is supported by the project: RDFORMING (reference PTDC/EME/31243/2017), co-funded by Portuguese Foundation for Science and Technology (FCT), by FEDER, through the program Portugal-2020 (PT2020), and by POCI, with reference POCI-01–0145-FEDER-031243. All supports are gratefully acknowledged.

References

[1] Chan LC, Kot WK. Determination of loading paths in warm hydroforming reinforced quadrilateral tubular components. Mater Manuf Process 2014;29:32–6.
[2] Saboori M, Champliaud H, Gholipour J, Gakwaya A, Savoie J, Wanjara P. Evaluating the flow stress of aerospace alloys for tube hydroforming process by free expansion testing. Int J Adv Manuf Technol 2014;72:1275–86.
[3] Ahmetoglu M, Sutter K, Li XJ, Altan T. Tube hydroforming: current research, applications and need for training. J Mater Process Technol 2000;98:224–31.
[4] Lang L, Wang Z, Kang D, Yuan S, Zhang S, Danckert J, Nielsen K. Hydroforming highlights: sheet hydroforming and tube hydroforming. J Mater Process Technol 2004;151:165–77.
[5] Bihamata R, D'Amours G, Bui QH, Guillot M, Raham A, Fafard M. Numerical and experimental studies on the new design concept of hydroforming dies for complex tubes. Mater Design 2013;47:766–78.
[6] Zribi T, Khalfallah A, BelhadjSalah H. Experimental characterization and inverse constitutive parameters identification of tubular materials for tube hydroforming process. Mater Design 2013;49:866–77.
[7] Hwang YM, Wang CW. Flow stress evaluation of zinc copper and carbon steel tubes by hydraulic bulge tests considering their anisotropy. J Mater Process Technol 2009;9:4423–8.
[8] Fuchizawa S, Narazaki M. Bulge test for determining stress-strain characteristics of thin tubes. In: Proceedings of the 4th ICTP advanced technology of plasticity; 1993. p. 488–93.
[9] Sokolowsky T, Gerke K, Ahmetgolu M, Altan T. Evaluation of tube formability and material characteristics: hydraulic bulge testing of tubes. J Mater Process Technol 2000;98:34–40.
[10] Liu J, Liu X, Yang LF, Liang H. Determination of flow stress of thin-walled tube based on digital speckle correlation method for hydroforming applications. Int J Adv Manuf Technol 2013;69:439–50.
[11] Song WJ, Kim J, Kang B. Experimental and analytical evaluation on flow stress of tubular material for tube hydroforming simulation. J Mater Process Technol 2007;19:368–71.
[12] Bortot P, Ceretti E, Giardini C. The determination of flow stress of tubular material for hydroforming for hydroforming applications. J Mater Process Technol 2008;203:381–8.
[13] Woo DM. Tube bulging under internal pressure and axial force. J Eng Mater Technol 1973;95:219–23.
[14] Koç M, Altan T. Application of two dimensional (2D) FEA for the tube hydroforming process. Int J Mach Tool Manuf 2002;42:1285–95.
[15] Manabe K, Amino M. Effects of process parameters and materials properties on deformation process in tube hydroforming. J Mat Process Technol 2002;123:285–91.
[16] Kridli GT, Bao L, Mallick PK, Tian Y. Investigation of thickness variation and corner filling in tube hydroforming. J Mater Process Technol 2003;133:287–96.
[17] Hwang YM, Chen WC. Analysis and finite element simulation of the tube expansion in rectangular cross-sectional die. Proceedings of the institution of Mechanical Engineers. Part B: J Engin Manuf 2003;217:127–35.
[18] Hwang YM, Chen WC. Analysis of tube hydroforming in square cross-sectional die. Int J Plast 2005;21:1815–33.
[19] Rama SC, Ma K, Smith LM, Zhang JM. A two-dimensional approach for simulation of hydroforming expansion of tubular cross-sections without axial feed. J Mater Process Technol 2003;141:420–30.
[20] Yuan SJ, Han C, Wang XS. Hydroforming of automative structural components with rectangular-sections. Int J Mach Tool Manuf 2006;46:1201–6.
[21] Orban H, Hu SJ. Analytical modelling of wall thinning during corner filling in structural tube hydroforming. J Mater Process Technol 2007;194:7–14.
[22] Xianghe X, Shuhui L, Weigang Z, Zhongqin L. Analysis of thickness distribution of square sectional hydroformed parts. J Mater Process Technol 2009;209:158–64.
[23] Xianghe X, Weigang Z, Shuhui L, Zhongqin L. Study of tube hydroforming in a trapezoid-sectional die. Thin-Walled Struct 2009;47:1397–403.
[24] Abdelkefi A, Guermazi N, Boudeau N, Malécot P, Haddar N. Effect of the lubrication between the tube and the die on the corner filling when hydroforming of different cross-sectional shapes. Int J Adv Manuf Technol 2016;87:1169–81.
[25] Abdelkefi A, Malécot P, Boudeau N, Guermazi N, Haddar N. Evaluation of the friction coefficient in tube hydroforming with the "corner filling test" in a square section die. Int J Adv Manuf Technol 2017;88:2265–73.
[26] Abdelkefi A, Malécot P, Boudeau N, Guermazi N, Haddar N. On the tube hydroforming process using rectangular, trapezoidal, and trapezoid-sectional dies: modeling and experiments. Int J Adv Manuf Technol 2017;93:1725–35.
[27] Venkateshwar Reddy P, Veerabhadra Reddy B, Janaki Ramulu P. An investigation on tube hydroforming process considering the effect of frictional coefficient and corner radius. Adv in Mater and Process Technol 2020;6:84–103.
[28] Barlat F, Brem JC, Yoon JW, Chung K, Dick RE, Choi SH, Pourboghrat F, Chu E, Lege DJ. Plane stress yield function for aluminium alloy sheets- Part I Theory. Int J Plast 2003;19(9):1297–319.
[29] Aretz H, Hopperstad OS, Lademo OG. Yield function calibration for orthotropic sheet metals based on uniaxial and plane tensile tests. J Mater Process Technol 2007;186:221–35.
[30] Grytten F, Holmedal B, Hopperstad OS, Borvik T. Evaluation of identification methods for YLD2004-18p. Int J Plast 2008;24:2248–77.
[31] Vrh M, Halilovic M, Starman B, Stok B, Comsa DS, Banabic D. Capability of the BBC2008 yield criterion in predicting the earing profile in cup deep drawing simulations. Euro J Mech A/Solids 2014;45:59–74.
[32] Jasson M, Nilsson L, Simonsson K. On constitutive modeling of aluminum for tube hydroforming applications. Int J Plast 2005;21:1041–58.
[33] Khalfallah A, Zribi T, Belhadjsalah H. A comparative study of the identification methods for tube hydroforming process. Key Eng Mater 2015;651-653:167–74.
[34] Xu Y, Chan LC, Tsein YC, Gao I, Zheng PF. Prediction of work hardening coefficient and exponential by adaptive inverse finite element method for tubular material. J Mater Process Technol 2008;201:413–18.
[35] Strano M, Altan T. An inverse energy approach to determine the flow stress of tubular materials for hydroforming applications. J Mater Process Technol 2004;104:92–6.
[36] Zribi T, Khalfallah A, Belhadjsalah H. Inverse method for flow stress parameter identification of tube hydroforming considering anisotropy. Int J Mech Manuf Syst 2011;4:441–53.
[37] Cazacu O, Barlat F. Generalization of Drucker's yield criterion to orthotropy. Math Mech Solids 2001;6:613–30.

[38] Rabahallah M, Balan T, Bouvier S, Bacroix B, Barlat F, Chung K, Teodosiu C. Parameter identification of advanced plastic strain rate potentials and impact on plastic anisotropy prediction. Int J Plast 2009;25:491–512.
[39] Alves JL, Oliveira MC, Menezes LF, Bouvier S. Influence of the yield criteria on the numerical results: cross tool example. In: Proceedings of the 9th international conference on material forming, Esaform'06, Glasgow, UK; 2006.
[40] Barlat F, Legev DJ, Brem JC. A six-component yield function for anisotropic materials. Int J Plast 1991;7:693–712.
[41] Khalfallah A, Oliveira MC, Alves JL, Menezes LF. Influence of the characteristics of the experimental data set used to identify anisotropy parameters. Simul Modell Pract Theory 2015;53:15–44.
[42] Wu PW, Jain M, Savoie J, MacEwen SR, Tugcu P, Neale KW. Evaluation of anisotropic yield functions for aluminum sheets. Int J Plast 2003;19:121–38.
[43] Menezes LF, Teodosiu C. Three dimensional numerical simulation of deep drawing process using solid finite element. J Mater Process Technol 2000;97:100–6.
[44] Neto DM, Oliveira MC, Alves JL, Menezes LF. Influence of the plastic anisotropy modelling in the reverse deep drawing process simulation. Mater Design 2014;6:368–79.
[45] Yi HK, Yim HS, Lee GY, Lee SM, Chung GS, Moon YH. Experimental investigation of friction coefficient in tube hydroforming. Trans Nonferrous Met Soc China 2011;21:194–8.
[46] Barrett Richard T. Fastener design manual. nasa. Scientific and Technical Information Division; 1990.
[47] Liu G, Yuan S, Teng B. Analysis of thinning at the transition corner in tube hydroforming. J Mater Process Technol 2006;177:688–91.
[48] Korkolis YP, Kyriakides S. Hydroforming of anisotropic aluminum tubes: part I experiments. Int J Mech Sci 2011;53:75–82.